Heliyon 10 (2024) e24412

Contents lists available at ScienceDirect

Heliyon

journal homepage: www.cell.com/heliyon

Research article

The mir-199b-5p encapsulated in adipocyte-derived exosomes mediates radioresistance of colorectal cancer cells by targeting JAG1

Xiaoli Lv [a,b,1], Zhenyan Li [a,b,1], Yunpeng Dai [a,b,1], Yuji Xiao [c], Fangrong Shen [d], Jian Wang [e], Jianping Cao [a,b], Lili Wang [f,***], Qiliang Peng [c,**], Yang Jiao [a,b,*]

[a] State Key Laboratory of Radiation Medicine and Protection, School of Radiation Medicine and Protection, Soochow University, Suzhou, 215123, China
[b] Collaborative Innovation Center of Radiological Medicine of Jiangsu Higher Education Institutions, Soochow University, Suzhou, 215123, China
[c] Department of Radiotherapy and Oncology, the Second Affiliated Hospital of Soochow University, Suzhou, 215004, China
[d] Department of Gynaecology and Obstetrics, the First Affiliated Hospital of Soochow University, Suzhou, 215006, China
[e] Department of Radiotherapy, the Affiliated Jiangyin People's Hospital of Nantong University, Jiangyin, 214400, China
[f] Department of Radiotherapy, the First Affiliated Hospital of Soochow University, Suzhou, 215006, China

ARTICLE INFO

Keywords:
Colorectal cancer
Radiosensitivity
Adipocyte
Exosome
miR-199b-5p
JAG1

ABSTRACT

Radiotherapy is a key treatment option for colorectal cancer, but its efficacy varies among patients. Our previous studies suggested that adipose tissue may confer the radioresistance of several abdominal tumors, such as pancreatic cancer, biliary cancer, and others. In the present work, the effects of adipocytes in regulating the radiosensitivity of colorectal cancer are explored for the first time. It was found that colony formation was increased and radiation-induced apoptosis decreased in colorectal cancer cells HCT8 and HCT116 co-cultured with adipocytes, which verified the mediation of adipocyte-driven radioresistance in colorectal cancer *in vitro*. Next, the colorectal cancer cells were incubated with adipocyte-derived exosomes, and a perceptible reduction in radiosensitivity was detected. Furthermore, to investigate the possible mechanisms involved, the exosomes were isolated, the encapsulated microRNAs were extracted and analyzed by small RNA sequencing. Based on bioinformatics analysis and qRT-PCR verification, miR-199b-5p was chosen for functional annotation. It was shown that miR-199b-5p expression was significantly upregulated after 6 Gy irradiation, and overexpressed miR-199b-5p significantly suppressed the radiosensitivity of HCT8 and HCT116 cells. In addition, jagged canonical Notch ligand 1(JAG1) was identified as the target gene of miR-199b-5p by using bioinformatics prediction and dual luciferase reporter gene assay. It was demonstrated that JAG1 conferred the radioresistance of colorectal cancer cells both *in vivo* and *in vitro*. Taken together, the present study demonstrates that adipocytes trigger the radioresistance of colorectal cancer cells, probably by targeting JAG1 through an adipocyte-derived exosomal miR-199b-5p.

* Corresponding author. State Key Laboratory of Radiation Medicine and Protection, School of Radiation Medicine and Protection, Soochow University, Suzhou, 215123, China.
** Corresponding author.
*** Corresponding author.
E-mail addresses: wanglili@suda.edu.cn (L. Wang), pengqiliang1912@163.com (Q. Peng), jiaoyang@suda.edu.cn (Y. Jiao).
[1] These authors contributed equally to this work.

https://doi.org/10.1016/j.heliyon.2024.e24412
Received 5 September 2023; Received in revised form 7 January 2024; Accepted 8 January 2024
Available online 10 January 2024

1. Introduction

According to the tumor statistics published by the International Agency for Research on Cancer (IARC), colorectal cancer has the third highest incidence and mortality rate of tumors worldwide [1]. The treatment measures normally include surgery, radiotherapy, and chemotherapy. Radiotherapy and chemotherapy are the main treatment for patients with advanced colorectal cancer [2]. However, many patients with colorectal tumors deal with the issue of insensitivity to radiotherapy [3], which seriously affects the survival rate of patients. As such, it is especially important to study the possible mechanism of resistance to radiotherapy in colorectal cancer patients.

Located in the abdominal cavity, colorectal tumors have a complex environment, which is infiltrated with a large number of adipocytes [4]. It has been reported that adipocytes play key roles in the development of various tumors [5–7]. For example, it was shown that adipocytes could facilitate the rapid growth of ovarian cancer by serving as an energy source [5]. In breast cancer, adipokines derived from adipocytes can promote the proliferation, angiogenesis, invasion and metastasis of the tumors [6]. In addition, we previously reported that adipocytes can enhance the tumor metastasis of cholangiocarcinoma, which might be related to the adipokines released from adipocytes [8]. However, the effects and mechanisms involved in the regulation of radiosensitivity of colorectal tumors by adipocytes have not yet been reported.

Exosomes are cell-derived micro vesicles, approximately 30–150 nm in diameter, that transport nucleic acids, proteins and lipids. They are released upon contact with the target cell surface, activating target cell-related signaling pathways and thereby mediating intercellular communication [9]. In the development of tumors, exosomes can regulate processes such as tumor immunity, tumor metastasis and tumor drug resistance [10]. Similarly, exosomes can regulate the development of colorectal tumors through the above-mentioned pathways [11]. MicroRNAs play an important role in the regulation of tumor development by regulating the expression of relevant target genes in tumor cells [12]. However, it remains unknown whether and how adipocyte-exosome derived miRNAs are involved in regulating the radiosensitivity of colorectal cancer.

In the present study, we found that miR-199b-5p of adipocyte exosome origin was significantly increased after 6 Gy X-ray irradiation, and one of the target genes was confirmed to be JAG1. Our study reported a possible mechanism of adipocytes to increase the radiation resistance of colorectal tumors, and provided a potential therapeutic target to improve the sensitivity of colorectal tumors to radiotherapy.

2. Materials and methods

2.1. Cell culture and irradiation

The colorectal cancer cell lines HCT8 and HCT116, utilized in our experiments, were acquired from Procell Life Science & Technology Co., Ltd. (Wuhan, China). These cell lines were cultured in RPMI 1640 Medium, enhanced with 10 % fetal bovine serum from Biological Industries and a 1 % penicillin-streptomycin solution from Beyotime Biotechnology (Shanghai, China). Culturing conditions involved a steady 37 °C temperature and a humidified environment with a 5 % CO2 concentration. To ensure optimal growth conditions, the medium was routinely replaced every alternate day. Irradiation of cells was performed by applying a 160 keV Rad Source X-ray generator (Suwanee, GA, USA), with a radiation field of 20 cm × 20 cm and dose rate of 1 Gy/min.

2.2. Human samples

Human adipose tissues were collected from the first affiliated hospital of Soochow University with the approval of the ethics committee of this institution (2022 Ethics Study Grant No.336). Written informed consents were obtained from all the participants.

2.3. Adipocyte isolation

0.2 % collagenase (Biofrox, Germany) and clipped human peri-intestinal adipocytes were added into a 50 mL centrifuge tube in a ratio of 3:1, and shaken at 37 °C for half an hour. After complete centrifugation, the fat was stratified: the upper layer was lipid, the middle layer was adipocytes, and the lower layer was fibrous connective tissue. The middle adipocyte layer was used for the experiments.

2.4. Exosomes isolation

Initially, adipocytes were gently aspirated, then relocated into separate co-culture chambers for further processing. These chambers, containing the adipocytes, were subjected to a 24-h incubation period in a medium devoid of serum. Subsequently, the first stage of centrifugation was carried out at a force of 300 g for a span of 10 min at a chilled temperature of 4 °C, aimed at separating the supernatant. This supernatant then underwent a secondary centrifugation at a higher force of 2000 g for an identical duration of 10 min, still maintaining the temperature at 4 °C. Post this step, the supernatant was meticulously filtered using a 0.22 μm filter. The resultant filtrate was then placed into an ultracentrifuge tube and subjected to a high-speed centrifugation at 35000 rpm (equivalent to 21000 g) for a period of 70 min, keeping the temperature constant at 4 °C. Following this, the upper layer of the supernatant was carefully removed, and PBS was introduced into the remaining substance. Another round of centrifugation was executed under

identical conditions. To conclude, the final supernatant was discarded, leaving behind a residue, which was then delicately combined with a small quantity of PBS through vortex mixing, facilitating the extraction of exosomes.

2.5. Colony formation assays

HCT8 and HCT116 cells were added to 6-well plates in a volume of 2 mL per well. After the cells were attached, they were incubated with an adipocyte co-culture or with exosomes for one day, and then irradiated with 0, 2, 4, 6, 8 Gy X-rays, respectively. Cells were transfected with miR-199b-5p mimics or shJAG1, then irradiated with 0, 2, 4, 6 and 8 Gy X-rays (400, 800,1200, 1600, and 2000 cells within the 0, 2, 4, 6, and 8 Gy groups, respectively). The cells were incubated for 14 days. In the final stage of the experiment, we treated the cells with a 4 % paraformaldehyde solution for fixation purposes, followed by a 20-min staining session at a standard room temperature using crystalline violet. This step was crucial for quantifying the cellular populations. For the analysis of cell survival trends, we employed the "single-hit multitarget" model. This involved calculating crucial metrics, notably the average fatal dose (D0) and the ratio indicating enhancement of sensitization (SER). These calculations were performed using the GraphPad Prism software, version 9.0 (provided by GraphPad Software), in alignment with previously established protocols [13].

2.6. Immunofluorescence assay

Assays were conducted according to the manufacturer's protocol as described previously [14]. Cells were incubated with γ-H2AX antibody (Abcam, UK) and Cy3-labeled goat anti-mouse IgG (Beyotime, China), followed by DAPI staining (Beyotime, China). Images were captured with an Olympus confocal microscope.

2.7. Flow cytometry apoptosis assay

HCT8 and HCT116 cell varieties were introduced into settings involving co-cultures with adipose tissue and exosome, or were subjected to transfection incorporating miR-199b-5p and shJAG1, maintained for 24 h. Subsequent to this, these cells were subjected to a 6 Gy dose of X-ray irradiation. At the 48-h mark following the irradiation, a process of centrifugation was employed to gather the cells, which were then suspended in a single strength buffer. The next step involved staining the cells, shielded from light, for a quarter of an hour using the Annexin V 7AAD/PE staining solution, a product of BD Biosciences based in the USA. The final step in the procedure was to conduct a flow cytometric analysis on the cells to evaluate the extent of apoptosis.

2.8. Small RNA sequencing and bioinformatics analysis

Total RNA extraction was performed on adipocyte extracellular vesicles, approximately 1 μL of the RNA sample was loaded onto an Agilent Technologies 2100 Bioanalyzer. The Bioanalyzer was employed to assess the size distribution and purity of the RNA sample, which are critical parameters for ensuring the integrity and suitability of RNA for small RNA sequencing. Subsequently, RT primers were employed, facilitating hybridization to prevent the self-ligation of any remaining 3′ adapters. This was followed by 5′ adapter ligation, succeeded by reverse transcription using random primers, effectively synthesizing the initial cDNA strand. PCR amplification was then carried out to enrich the library and introduce sequencing and index sequences, essential for subsequent data analysis. Target library fragments (138-160bp) were meticulously selected via PAGE gel electrophoresis. Ensuring library quality, we assessed size distribution using the Agilent 2100 Bioanalyzer and quantified library concentration through Qubit 3.0 or fluorescence-based PCR methods. Ultimately, the libraries underwent pooling and were subsequently subjected to high-throughput sequencing, marking the culmination of our experimental process. For bioinformatics predictions, differentially expressed miRNAs were initially identified using DESeq software, based on fold-change criteria and the negative binomial distribution test. In the subsequent small RNA sequencing analysis, for samples lacking biological replicates, the Audic_Claverie formula was employed to calculate p-values, whereas for those with biological replicates, the DEG algorithm within the R package was utilized. miRNAs with p-values less than 0.05 were selected for further analysis. Additionally, for the KEGG and GO enrichment analyses of miRNA targets, the hypergeometric distribution test in R was applied, and p-values were adjusted using the Benjamini & Hochberg method to derive the False Discovery Rate (FDR). These experiments were conducted at OE Biotech, Shanghai, China.

2.9. Dual luciferase assay

Experimental kits were provided by Promega (Beijing, China). Renilla luciferase activity was used to normalize the relative luciferase activity. The plasmids used in the experiments were supported by Ribobio, (Guangzhou, China). The sequences of the plasmids were: 135–141 of JAG1-WT: 5'- ….UUGACAAGCUGGCUUACACUGGC ….-3'; 135–141 of JAG1-MUT: 5'- ….UUGACAAGCUGGCUUTGTGACCC ….-3'.

2.10. RNA extraction and quantitative real-time PCR

Total RNA was extracted from HCT8 and HCT116 cells using the RNA-Quick Purification Kit (ES science, Shanghai, China), the quantity and quality of extracted RNA were assessed using a NanoDrop spectrophotometer (Thermo, USA). And mRNA was reverse transcribed using the All-In-One 5× RT MasterMix (ABMGood, Guangzhou, China). Real-time PCR was performed using NovoStart

SYBR qPCR SuperMix plus (Novoprotein, Shanghai, China). The primers used were as shown in Table 1.

2.11. Bioinformatic analysis

Expression data for miR-199b-5p and JAG1 in colorectal cancer was sourced from the TCGA (The Cancer Genome Atlas) database. Initially, this RNAseq data, provided in FPKM format, was converted to TPM format. This data was then subjected to log2 transformation in preparation for statistical examination. The R software environment was used for this analysis. To compare expression levels in cancerous tissues against those in normal tissues, the Kruskal-Wallis test was applied. All statistical evaluations were performed using R software, with visualization of the outcomes facilitated by the 'ggplot2' package.

2.12. Western Blot

Lysis of HCT8 and HCT116 cells was carried out utilizing RIPA lysis buffer. Subsequent determination of protein concentrations in the lysates was conducted using the BCA Protein Assay kit (Beyotime, China). Specific steps for the Western blot experiment were conducted in accordance with the protocols outlined in our previously published article [15]. After chemiluminescence, the target bands and the internal reference (GAPDH or α-Tubulin) were quantified by Image J software.

In this study, the following antibodies were employed: anti-γ-H2AX (Cell Signaling Technology, USA; 9718S, 1:1000); anti-TSG101 (Cell Signaling Technology, USA; 28405S, 1:1000); anti-CD9 (Cell Signaling Technology, USA; 98327S, 1:1000); anti-GAPDH (Cell Signaling Technology, USA; 5174S, 1:1000); anti-α-Tubulin (Cell Signaling Technology, USA; 2125S, 1:1000).

2.13. Transfection assay

MiR-199b-5p mimics, its inhibitor, and JAG1-targeted short hairpin RNAs (termed shJAG1) were custom-designed and synthesized by WZ Biosciences (Jinan, China). For transfection into HCT8 and HCT116 cell lines, a concentration of 10 nM of these mimics and inhibitors was used, employing Lipofectamine RNAi MAX as the transfection agent (Invitrogen, USA), or transfected with 10 nM shRNAs using Lipofectamine 3000 (Invitrogen, USA). The culture medium was changed 8 h after transfection. The miR-199b-5p mimics, inhibitors and shJAG1 sequences used were as shown in Table 2.

2.14. Xenograft experiments

Male nude mice, aged six weeks, were procured from SLAC Laboratory Animal Co., Ltd., located in Shanghai, China. These mice were raised in an environment free from specific pathogens, in line with the guidelines for animal care established by Soochow University. The mice resided in a habitat where the temperature was consistently maintained between 24 °C and 26 °C, and the humidity levels were kept close to 50 ± 5 %. The light and dark periods were alternated every 12 h in their living space, ensuring they had continuous access to sterilized food and water. All procedures involving these mice were meticulously carried out, respecting the ethical standards and animal care practices as prescribed by the Research Ethics Committee of Soochow University and the norms for Laboratory Animal Care and Use.

First, 1×10^7 HCT8 and HCT116 cells were subcutaneously injected into male BALB/c nude mice (4 weeks old). When the volume of the tumors reached 100 mm^3, HCT8 and HCT116-derived tumors were divided into two groups, with one group receiving an injection of exosomes and the other group receiving an equal amount of PBS (100 μg) 24 h and 2 h before 10 Gy X-rays radiotherapy. The radiotherapy of xenografts was performed by using a 160 keV RadSource irradiator (Suwanee, GA, USA) with a dose rate of 1 Gy/min. The tumor volume was calculated as (length × $width^2$)/2. Finally, tumor tissues were removed and analyzed.

2.15. Hematoxylin-eosin (HE) staining

Tissue samples from tumors underwent fixation using 4 % formaldehyde, followed by a dehydration process and clearing with alcohol and xylene. They were then embedded into paraffin blocks. The embedded tissues were sectioned and stained; hematoxylin was used for staining the nuclei, and eosin for the cytoplasm. Post-staining, these sections were again dehydrated using alcohol, cleared with xylene, and finally mounted using resinene. Microscopic examination and photography of these prepared sections were then performed. Tumor tissues were fixed with 4 % formaldehyde, dehydrated and made transparent with alcohol and xylene, embedded

Table 1
List of primer sequences of related RNAs.

RNA	Forward	Reverse
miR-199b-5p	CCCAGTGTTTAGACTATCTGTTC	GTTGATGTTGAGAAGCCTTGTC
JAG1	ATTACCAGGATAACTGTGCGAA	CAAATGTGCTCCGTAGTAAGAC
CCNL1	CGTCAAACACAGTTTCGAGATT	GTCCTTTTTCCTCTTAACTGGC
NLK	TGAATCCCGTCATATGACTCAG	GATCCGTGATCAAATCCAACTG
HIF1A	AGTTCCGCAAGCCCTGAAAGC	GCAGTGGTAGTGGTGGCATTAGC
TAF9B	GTTGATGCAGATGATGTGAGAC	ATTTTTCTGCCTTGCGATATCC

Table 2
List of sequences of miR-199b-5p mimics, inhibitors and shJAG1.

	Sequences
mimic-nc	CCCAGTGTTTAGACTATCTGTTC
inhibitor-nc	ATTACCAGGATAACTGTGCGAA
mimic-miR199b-5p	CGTCAAACACAGTTTCGAGATT
inhibitor-miR-199b-5p	TGAATCCCGTCATATGACTCAG
shJAG1	GTGCACCTCTGACTCCTATTATTCAAGAGATAATAGGAGTCAGAGGTGCACTTTTTT-

with wax blocks, sectioned and thereafter stained with hematoxylin for nuclei and eosin for the cytoplasm. After staining, the sections were dehydrated with alcohol and then made transparent with xylene. The sections were sealed with resinene and subsequently observed under a microscope and photographed.

2.16. Co-immunoprecipitation (Co-IP)

Total proteins were extracted from HCT8 and HCT116 cells using RIPA buffer supplemented with protease and phosphatase inhibitors. For Co-Immunoprecipitation, pre-cleared lysates were incubated overnight at 4 °C with anti-JAG1 or anti-NOTCH1 antibodies conjugated to Protein A/G PLUS-Agarose beads. Post washing to remove non-specifically bound proteins, the immunocomplexes were analyzed by SDS-PAGE followed by immunoblotting, employing the same anti-JAG1 and anti-NOTCH1 antibodies to detect the interaction between these proteins.

2.17. Statistical significance

Statistical analysis was carried out using the 9.0 version of GraphPad Prism, developed by GraphPad Software, Inc. in La Jolla, CA, USA. The results were expressed as means along with their respective standard errors of the mean (SEM). For evaluating the differences between distinct groups, we utilized a one-way ANOVA, followed by a Tukey's test for post hoc comparisons. We standardly performed each experiment three times independently, unless otherwise mentioned. A *P*-value below 0.05 was treated as a threshold for deeming results as statistically significant.

3. Results

3.1. Adipocytes increase radioresistance of colorectal cancer cells

HCT8 and HCT116 cells were cultured in the lower layer of 8 μm transwell while adipocytes were cultured in the upper layer of the chambers. These were co-cultured for 24 h, then irradiated with 0, 2, 4, 6 and 8 Gy X-rays. As shown in Fig. 1A, HCT8 cells showed radiation resistance after co-culture with adipocytes, with higher survival fractions (SF) at 2, 4, 6, and 8 Gy, and the sensitizer enhancement ratio (SER) value was 0.95(Table 3). HCT116 cells seemed to be more sensitive to radiation, with almost no survival after co-culture with adipocytes after 6, and 8 Gy X-ray irradiation, but at 2, and 4 Gy irradiation, the SF was 0.15 and 0.0022 for the irradiated group alone, 0.32 and 0.072 for the co-cultured group with adipocytes. Both groups recorded higher SFs. After 6 Gy X-ray irradiation, immunofluorescence results showed that the expression of DNA damage repair protein γ-H2AX was significantly reduced (Fig. 1B). Western blot analysis showed that γ-H2AX was also down-regulated especially at 0.5 and 2 h after irradiation (Fig. 1C). The apoptosis rate of HCT8 cells after co-culture at 48 h after irradiation was significantly lower compared to the irradiation group alone (Fig. 1D). These results indicate that co-culture with adipocytes can significantly reduce the radiosensitivity of colorectal cancer HCT8 and HCT116 cells.

3.2. Exosomes derived from adipocytes increase radioresistance of colorectal tumor cells

To investigate the possible mechanisms of adipocytes in modulating the radiosensitivity of colorectal tumor cells, exosomes were first extracted from adipocytes and examined using electron microscopy and expression of exosomal marker proteins TSG101 and CD9 (Fig. 2A–C). The uptake of exogenous exosomes by colorectal tumor cells was then detected by immunofluorescence, and the results showed a gradual increase in the entry of exosomes into the cells over time (Fig. 2D). Subsequent colony formation experiments confirmed that the addition of exosomes significantly enhanced the rate of colony formation after different doses of irradiation. The SER value was 0.94 in HCT8 cells (Table 3). In HCT116 cells the SF of 2, and 4 Gy was 0.14 and 0.012 for the irradiated group alone; 0.30 and 0.031 for the exosomes group (Fig. 2E). The addition of exosomes also reduced the rate of apoptosis induced by 6 Gy X-ray irradiation (Fig. 2G), while WB and immunofluorescence experiments confirmed that the expression of γ-H2AX was significantly reduced in the group with the addition of exosomes (Fig. 2F). In the *in vivo* experiment, the growth rate of HCT8 tumor volume after radiotherapy with exosome injection was slower than that of the radiotherapy alone group, but there was no significant difference ($p > 0.05$). While there was no significant difference in HCT116 tumor volume at 3, 6 and 9 days after radiotherapy, and at 12 and 15 days, the tumor volume of the radiotherapy alone group was significantly smaller than that of the exosome injection group ($p < 0.05$), indicating that exosomes could significantly reduce the sensitivity of colorectal tumors to radiotherapy (Fig. 2H). Histopathological

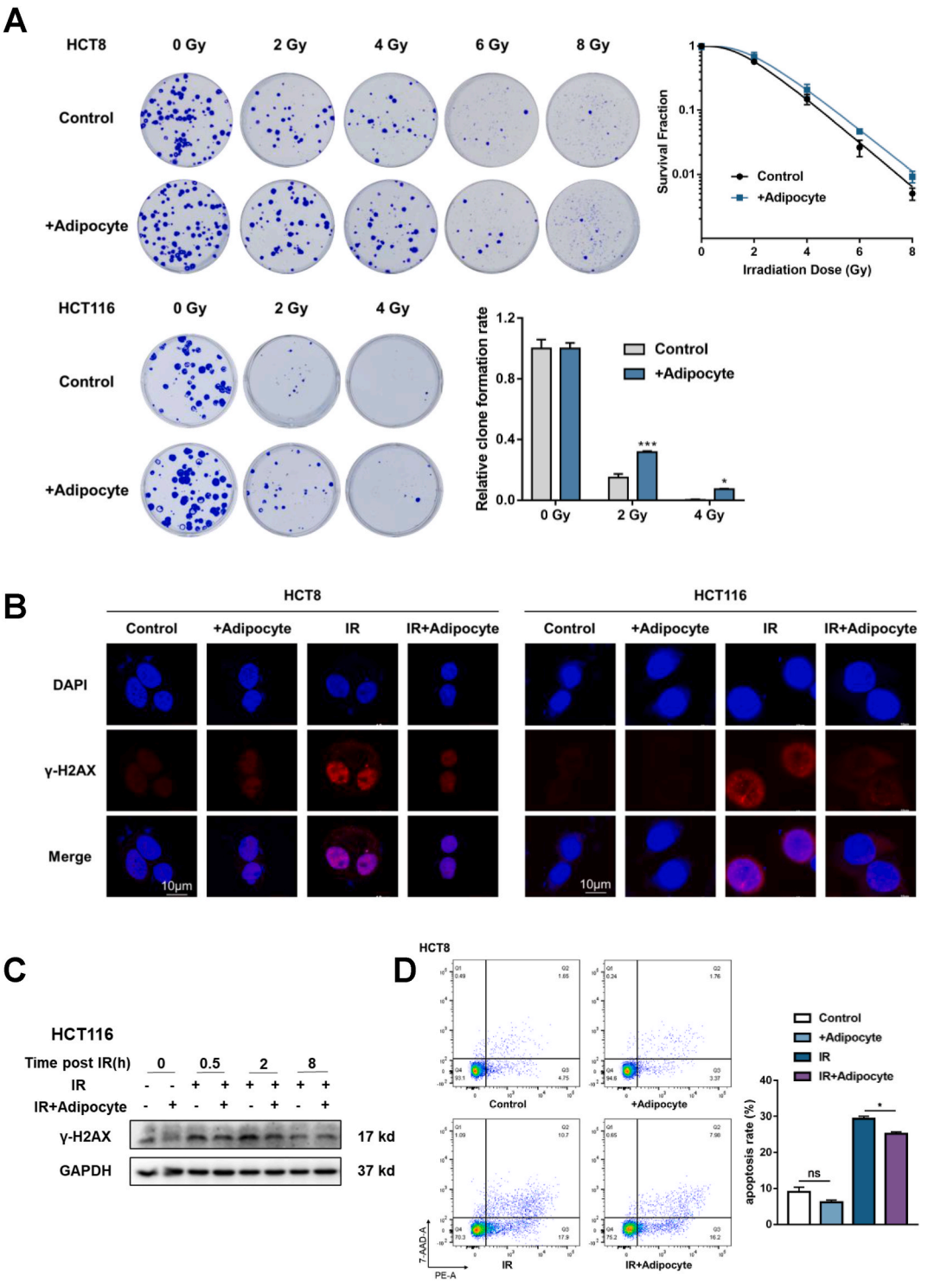

(caption on next page)

Fig. 1. Adipocytes increase radioresistance in colorectal cancer cells. (A) Displayed are typical colony formation images and corresponding survival curves for colony formation assays in HCT8 and HCT116 cells. (B) Showcased are confocal immunofluorescence stained images of HCT8 and HCT116 cells, with γ-H2AX marked in red and nuclei stained blue using DAPI. (C) Western Blot (WB) analysis was employed to assess the γ-H2AX protein levels in cells that were both co-cultured with adipocytes and subjected to radiation, in comparison to a control group that received only irradiation. (D) The apoptotic rates in HCT8 cells were determined using flow cytometry, where the lower left quadrant represents viable cells, early apoptosis is indicated in the lower right quadrant, and late apoptosis is shown in the upper right quadrant. The total apoptosis count encompasses both early and late stages of apoptosis, and the analysis of apoptosis rates in both HCT8 and HCT116 cells was conducted. These findings are based on mean values derived from three independent experiments, and the statistical evaluation was performed using a one-way ANOVA. *$p < 0.05$, **$p < 0.01$, ***$p < 0.001$.

Table 3
The D0, N and SER values of cells treated with different treatment conditions. The SER value was simulated using the multi-target single hit model.

Cell	Group	D0	N	SER
HCT8	Control	1.257	3.724	0.945
	+Adipocyte	1.330	4.571	
	Control	2.979	0.673	0.939
	+Exosome	3.171	0.916	
	mimic-nc	1.341	4.148	0.853
	mimic-miR199b	1.572	5.955	
	shNC	1.091	2.231	0.974
	shJAG1	1.120	3.437	
HCT116	mimic-nc	1.764	1.347	0.831
	mimic-miR199b	2.124	1.273	
	shNC	0.724	3.143	0.673
	shJAG1	1.076	1.706	

staining on the tumor tissue showed nuclear aggregation, deep nuclear staining and other significant features of tumors (Fig. 2I). These results indicate that tumor cell-derived exosomes can significantly reduce the radiosensitivity of colorectal tumor cells both *in vivo* and *in vitro.*

3.3. Exosome-encapusulated mir-199b-5p mediates the radioresistance of colorectal tumor cells

In order to investigate the possible mechanism whereby microRNA in exosomes regulate colorectal tumor cell sensitivity to radiotherapy, high-throughput sequencing of miRNAs in exosomes from adipocytes obtained from patients before and after radiotherapy was performed, in which 14 miRNAs were significantly different after radiotherapy (Fig. 3A). These 14 miRNAs selected by sequencing were further validated by RT-qPCR experiments, which showed that miR-199b-5p was significantly elevated after 6 Gy X-ray irradiation (Fig. 3B). Initially, analysis of TCGA database for colorectal cancer revealed that miR-199b-5p expression was significantly higher in tumor tissues compared to adjacent non-tumoral tissues in both matched and unmatched samples (Fig. S1A). Concurrently, the expression of miR-199b-5p was evaluated in human normal intestinal epithelial cells (HIEC), as well as in HCT8 and HCT116 colorectal cancer cells. Notably, a marked elevation in miR-199b-5p expression was observed in colorectal cancer cells relative to normal intestinal epithelial cells (Fig. S1B). This prompted further investigation into the role of miR-199b-5p in influencing the radiosensitivity of colorectal tumors. After miR-199b-5p mimics transfection (Fig. S1C), HCT8 and HCT116 cells were irradiated with 2, 4, 6 and 8 Gy X-rays, the SER values were found to be 0.85 and 0.83 in HCT8 and HCT116 cells (Fig. 3C–Table 3). Meanwhile, the apoptotic rate of cells in the group transfected with miR-199b-5p mimics was significantly lower than that of the simple irradiation group after 6 Gy X-ray irradiation (Fig. 3D). Immunofluorescence and WB experiments confirmed that γ-H2AX protein expression was also significantly lower than that of the simple irradiation group (Fig. 3E and F). TCGA database showed lower miR-199b-5p expression in colorectal tumor patients treated with additional radiotherapy than in those who did not receive it ($p = 0.0032$) (Fig. 3G). Furthermore, Kaplan-Meier survival analysis reveals that high miR-199b-5p expression correlates with shorter disease specific survival (DSS) in colorectal cancer patients ($p = 0.0101$, Fig. 3H), while it shows no significant effect on overall survival (OS) ($p = 0.492$, Fig. S1D). These results confirmed that miR-199b-5p significantly reduced the radiosensitivity of colorectal tumor cells.

3.4. miR-199b-5p regulates the radiosensitivity of colorectal cancer cells by targeting JAG1

To further evaluate the specific mechanism by which miR-199b-5p regulates the sensitivity of colorectal tumor cells to radiotherapy, five possible target genes of miR-199b-5p were selected through the database (Fig. S2A). Subsequently, by detecting the changes in target gene expression after transfection with miR-199b-5p (Fig. 4A), JAG1 was identified as an miR-199b-5p target gene using a dual luciferase gene reporter assay. Fig. 4B and C showed the predicted binding sites in miR-199b-5p and the 3′-UTR of JAG1. JAG1 is upregulated after different doses of irradiation and has a time-dependent expression after 6 Gy irradiation (Figs. S2B and C). By transfecting plasmids shNC and shJAG1 in HCT8 and HCT116 cells (Fig. S2D), which were subjected to 2, 4, 6 and 8 Gy X-ray irradiation, and SER values of 0.97 and 0.67, we showed that shJAG1 could significantly increase the rate of colony formation (Fig. 4D–Table 3). In addition, JAG1 knocked down before 6 Gy X-ray irradiation, significantly reduced the apoptotic rate of shJAG1

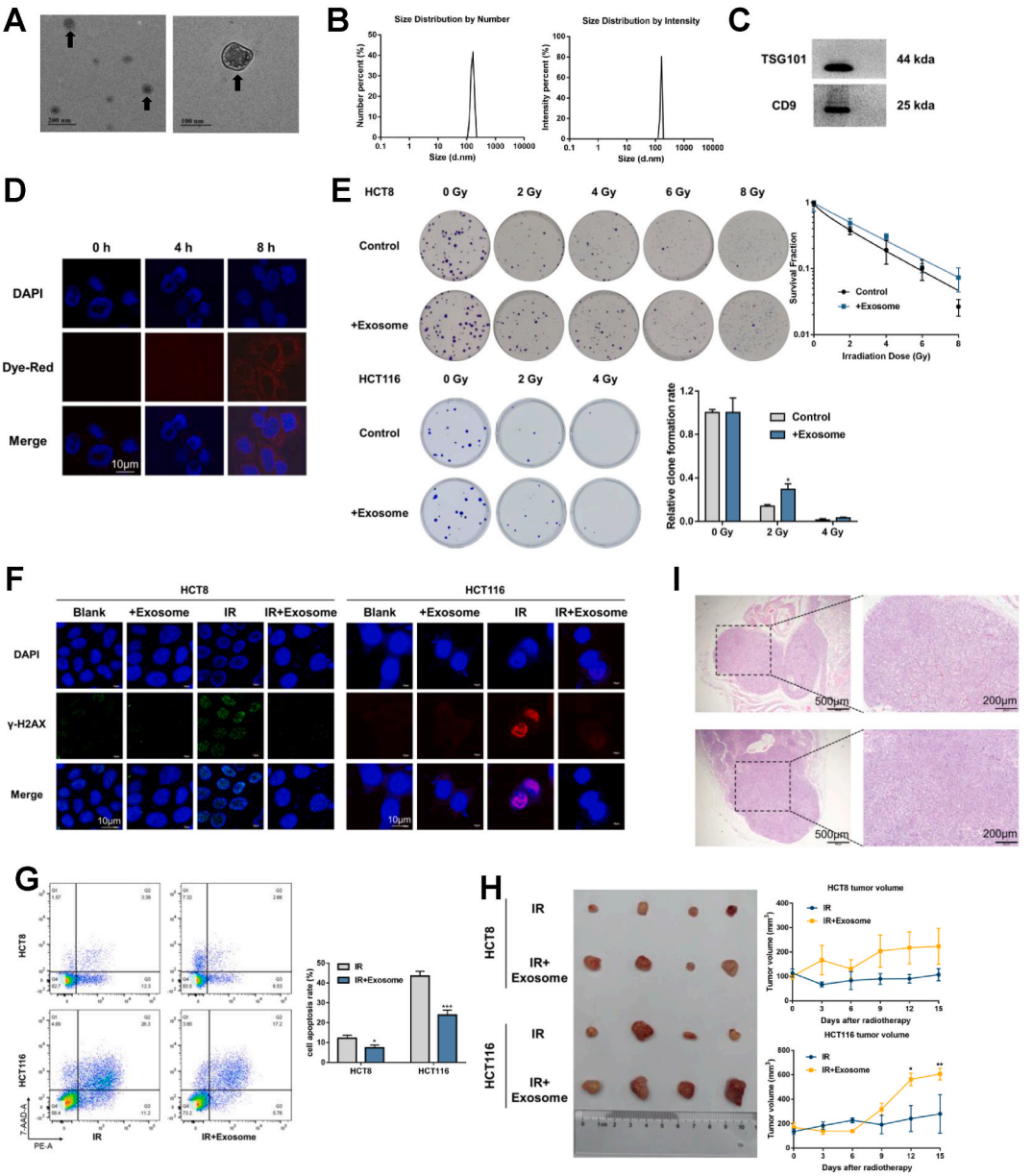

Fig. 2. Exosomes derived from adipocytes increase radioresistance of colorectal cancer cells. (A) Scanning electron microscope images representative of exosomes, black arrows indicate representative exosomes. (B) Nanoparticle tracking analysis by Nano Sight. (C) WB was employed to identify standard exosomal biomarkers in HCT8 cells. (D) An immunofluorescence technique was utilized to observe temporal alterations in cell uptake following the introduction of exosomes, with exosomes marked using Dye-red and cell nuclei counterstained with DAPI in blue. (E) Displayed are characteristic images of colony formations and the associated survival curves from colony formation assays in HCT8 and HCT116 cells. (F) Confocal immunofluorescence staining was conducted on HCT8 and HCT116 cells, highlighting γ-H2AX in either green or red, while the nuclei were stained blue using DAPI. (G) The apoptotic levels in HCT8 and HCT116 cells were assessed using flow cytometry, where cells in the lower left quadrant represent the living, those in the lower right indicate early apoptosis, and cells in the upper right signify late apoptosis. The cumulative apoptosis includes both early and late stages. A detailed statistical analysis of the apoptosis rates in these cells is also provided. (H) Observational analysis of tumor development in HCT8 and HCT116 cells was conducted post-carcinogenesis, following exclusive radiotherapy and after radiotherapy coupled with exosome injection in each respective group. Tumor dimensions were measured daily and computed using formula $V = 1/2\ ab^2$ (where 'a' is length and 'b' is width). (I) Hematoxylin and Eosin (HE) staining was applied for the histological examination of the tumor tissues. *p < 0.05, ****p < 0.0001, using two-way ANOVA.

cells (Fig. 4E). To further elucidate this relationship, we introduced a miR-199b-5p inhibitor into shJAG1 cell lines, which resulted in the re-expression of JAG1. Subsequent analyses revealed an increased rate of apoptosis in HCT8 and HCT116 cell lines, in comparison to those transfected with miR-199b-5p nc (Fig. 4F). Subsequent analysis within the TCGA colorectal cancer dataset revealed a negative

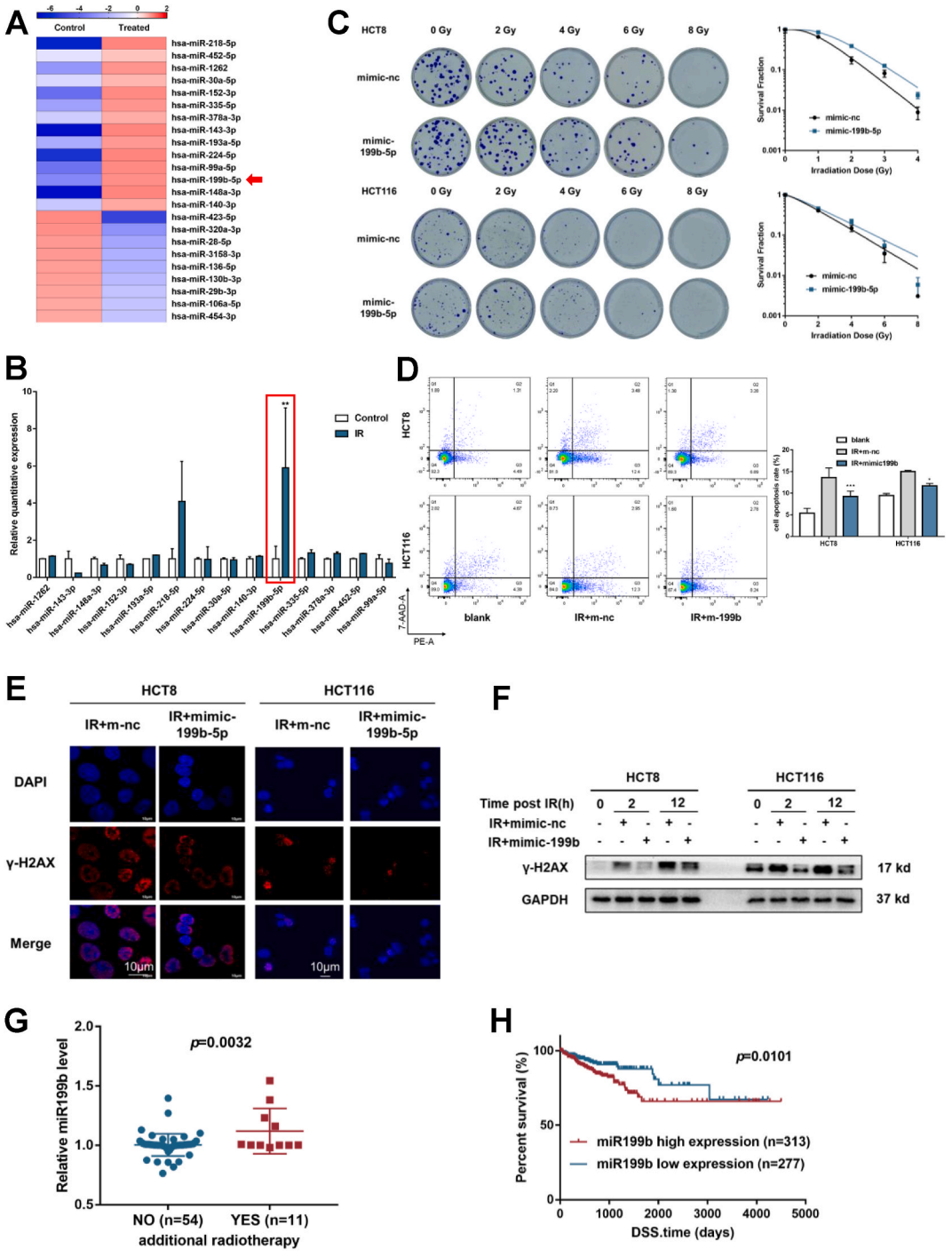

(caption on next page)

Fig. 3. miR-199b-5p derived from exosomes reduces the radiosensitivity of colorectal cancer cells. (A) Heat map display of miRNA changes after radiotherapy. (B) RT-qPCR validation of exosome-derived miRNA expression after 6 Gy irradiation. (C) Displayed are select images demonstrating colony formations and their corresponding survival curves from the colony formation assays conducted on HCT8 and HCT116 cell lines. (D) Apoptotic rates in both HCT8 and HCT116 cells were quantified using flow cytometry. In the analysis, cells in the lower left quadrant are indicative of live cells, those in the lower right quadrant suggest early stage apoptosis, while cells in the upper right quadrant signal late stage apoptosis. The overall apoptosis rate encompasses both the early and late phases of apoptosis. A detailed statistical breakdown of these apoptosis rates in both cell lines is included. (E) The confocal immunofluorescence staining images of HCT8 and HCT116 cells are showcased, where γ-H2AX is marked in red, and the cell nuclei are distinctly stained in blue with DAPI. (F) The expression of γ-H2AX protein in miR-199b-5p up-regulated irradiated group and control irradiated group were analyzed by WB. (G) TCGA database shows miR-199b-5p expression in colorectal cancer patients after additional radiotherapy. (H) TCGA database demonstrates the relationship between high or low expression of miR-199b-5p and survival of colorectal cancer patients. Data are expressed as the means from 3 separate experiments, and statistical analyses were performed using one-way ANOVA. *$p < 0.05$, **$p < 0.01$, ***$p < 0.001$.

correlation between miR-199b-5p and JAG1 expression, although this association was not statistically significant ($p = 0.520$, $R = -0.026$) (Fig. S2E). Additionally, the correlation between JAG1 expression and overall survival (OS) in colorectal cancer patients was also analyzed, yielding no significant association ($p = 0.309$) (Fig. S2F). These findings indicate that miR-199b-5p plays a pivotal role in modulating the radiosensitivity of colorectal cancer cells, primarily through its interaction with JAG1.

4. Discussion

Improving the sensitivity of colorectal cancers (CRC) to radiotherapy is important for prolonging the survival of patients and improving their quality of life. Due to the differences among individual patients, we found that adipocytes can significantly reduce the sensitivity of colorectal tumors to radiotherapy. Based on this, we investigated the possible mechanisms by which adipocytes modulate the sensitivity of colorectal tumors to radiotherapy, providing a potential therapeutic target for improving the sensitivity of colorectal tumor patients to radiotherapy.

The mechanisms that regulate the sensitivity of colorectal tumors to radiotherapy are complex, and the role of adipocytes in this regulation was identified in another unpublished study of our group. Adipocytes, however, are often thought to be a source of energy, providing a large amount of energy that plays a role in the development of cancers [16]. It has been experimentally demonstrated that tumor growth rates are significantly higher in fat-rich environments than in low-fat locations, however, whether fat regulates the development of cancers through other pathways besides providing energy is being increasingly explored by researchers. Meanwhile, more and more studies have found that the endocrine role of adipocytes plays an important role in regulating metabolism, apoptosis and other physiological processes in cancer cells. A study by Qi Wu suggested that cancer associated adipocytes, besides having a direct effect on cancer cells, systematically prepares the microenvironment by promoting anti-cancer immunity [17]. However, the role of adipocytes in colorectal cancer radiotherapy still needs further study. We simulated the lipid-rich environment of colorectal tumors in our preliminary experiments, and found that the co-culture of colorectal tumor cells and adipocytes could significantly reduce the sensitivity of colorectal tumor cells to radiotherapy. Further studies are still needed on the mechanism of adipocyte regulation of colorectal tumor sensitivity to radiotherapy.

Adipocytes act as endocrine cells to regulate the physiological behavior of tumors by secreting certain substances that are transported through blood, interstitial fluid and lymphatic fluid which subsequently act on the target cells. Exosomes, as one of the important modes of external communication by adipocytes, play an indispensable role in regulating the physiological processes in tumor cells. It is usually believed that adipocytes secrete exosomes in the form of cytosol, and alter cytokinesis by tumor cells, the genetic material within exosomes is secreted and acts within the tumor. In the development of colorectal tumors, genetic information can act on tumor proliferation, metastasis and drug resistance through exosomal transmission, but the source of exosomes is mostly secreted by the tumor itself, while the regulation of tumor behavior by adipocytes through the exosomal pathway has not been confirmed by studies. In our previous experiments, we found that the radiation resistance of tumor cells was significantly increased after the addition of adipocyte-derived exosomes to colorectal tumor cells, while the radiation-induced tumor suppression was significantly alleviated by the advance injection of adipocyte-derived exosomes into nude mouse tumor bodies. Our results suggest that exosomes play an important role as a mediator in adipocyte regulation of radiosensitivity in CRC, but the informative substances transported by exosomes which modulate the radiosensitivity of cancer cells still needs to be investigated further.

Exosomes are membranous vesicles released into the extracellular matrix through fusion of intracellular multivesicular bodies with the cell membrane, and usually encapsulate proteins, mRNA, and non-coding RNAs, which are picked up by the target cells and released to regulate the biological behavior of the target cells. Since exosomes are formed in the cytoplasm, the non-coding RNAs encapsulated in them play an important role in regulating the biological behavior of cancer cells. Many studies have now confirmed that exosomes carrying miRNAs can regulate cancer cells. miR-199b-5p, which may play a role, has been screened in our previous study by sequencing miRNA before and after clinical radiotherapy and verified by RT-qPCR. miR-199b -5p has been studied previously. Research by Zhigang Zhao found that miR-199b-5p targets DDR1 to regulate the EMT process, which in turn regulates the aggressive metastatic ability of prostate cancer [18]. In another study, miR-199b-5p was shown to regulate the progression of gastric cancer by targeting HHIP [19]. While the function of miR-199b-5p in CRC has not been reported, our previous experiments confirmed that irradiation significantly upregulated miR-199b-5p expression in colorectal cancer cells HCT8 and HCT116. In addition, overexpression of miR-199b-5p by lentiviral infection of cancer cells significantly increased the rate of clone formation of cancer cells after irradiation and decreased radiosensitivity. Moreover, recent research has revealed that miR-6716-5p promotes metastasis in colorectal cancer by

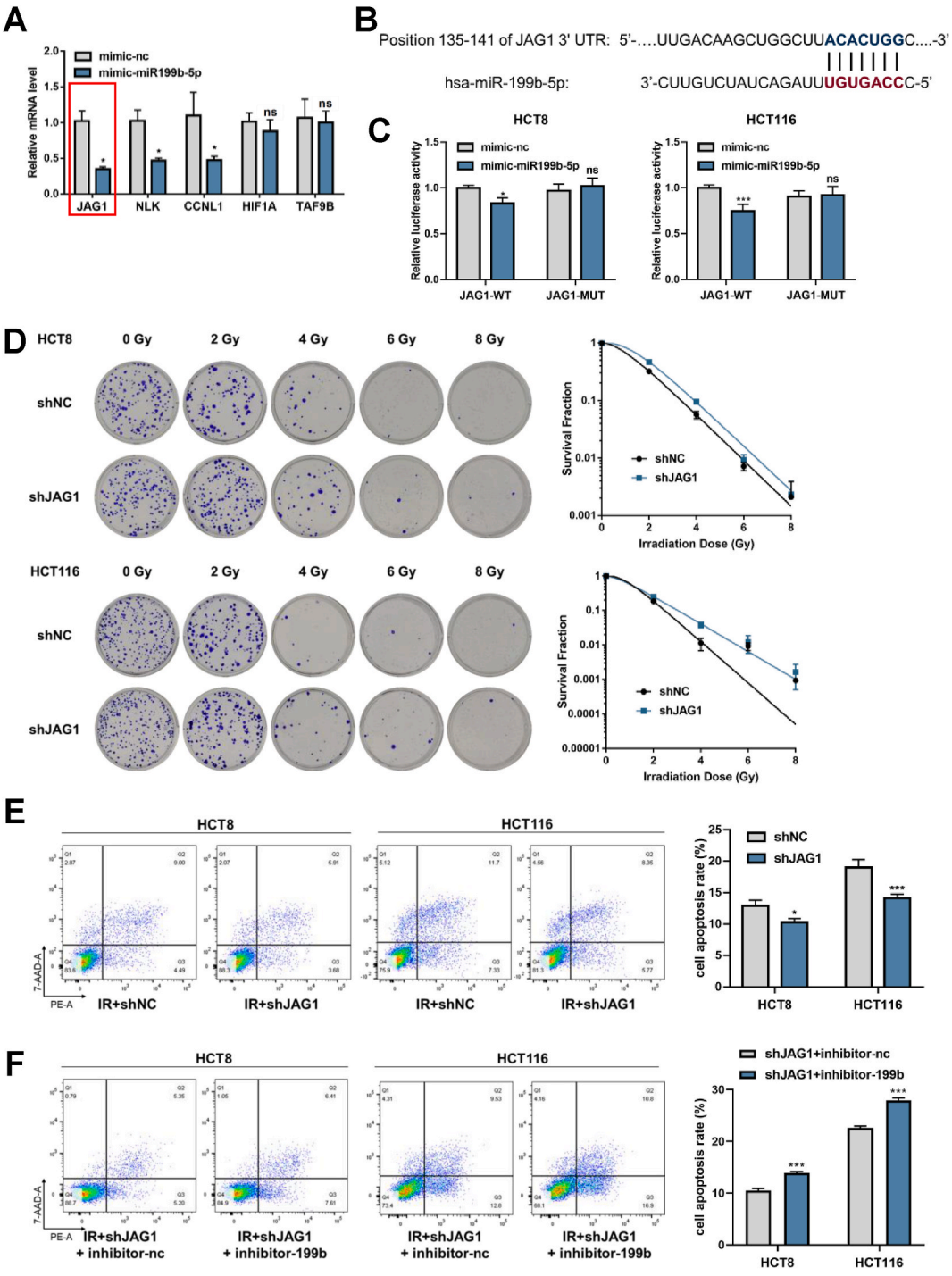

Fig. 4. miR-199b-5p derived from exosomes reduced the radiosensitivity of colorectal cancer cells. (A) Expression of possible target genes after upregulation of miR-199b-5p detected by qRT-PCR. (B) Schematic representation of the possible binding site of miR-199b-5p to the 3′UTR of JAG1. (C) Dual luciferase assays detect upregulated miR-199b-5p, and luciferase activity after 3′UTR mutation of JAG1 in HCT8 and HCT116 cells. (D) Knock down of JAG1 followed by irradiation of 0, 2, 4, 6 and 8Gy X-rays. Representative images of colony formation and survival curve of the colony formation assay of HCT8 and HCT116 cells are presented. (E) Knock down of JAG1 followed by irradiation of 6 Gy X-rays. (F) Transfection of miR-199b-5p inhibitor in shJAG1 cells, followed by exposure to 6 Gy X-ray irradiation. Apoptotic levels in HCT8 and HCT116 cells were assessed through flow cytometry. In this method, viable cells are identified in the lower left quadrant, cells undergoing early apoptosis are noted in the lower right quadrant, and those in late apoptosis are marked in the upper right quadrant. The aggregate of early and late apoptosis forms the total apoptosis count. The apoptosis rates for both HCT8 and HCT116 cells were analyzed statistically. The results shown represent the average of three distinct experiments, and a one-way ANOVA was utilized for the statistical evaluation. *$p < 0.05$, **$p < 0.01$, ***$p < 0.001$.

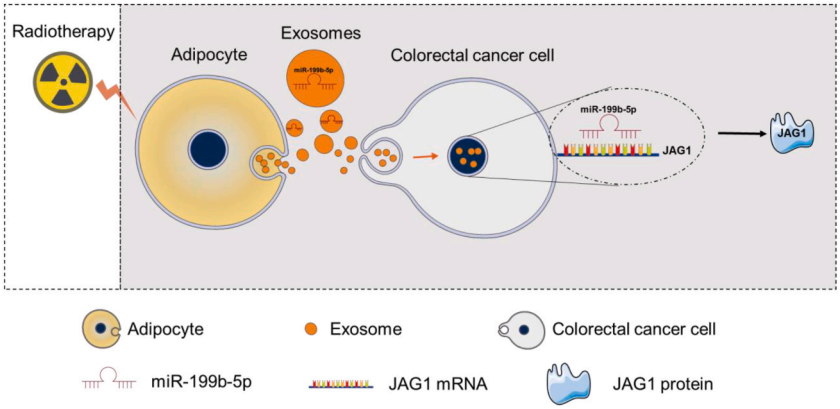

Fig. 5. A graphical summary of exosome encapsulated miR-199b-5p from adipocytes mediating the radioresistance of colorectal cancer cells by targeting JAG1.

downregulating NAT10 expression, indicating its potential as a therapeutic target [20]. This finding underscores the profound and extensive role of miRNAs in colorectal tumors, meriting in-depth investigation.

In the investigation into the specific mechanism by which miR-199b-5p regulates cancer radiosensitivity, JAG1 was confirmed as the target gene of miR-199b-5p originally through prediction site screening, followed by qRT-PCR assay, and dual luciferase assay for validation. JAG1 acts as a ligand for Notch by binding to it. The Notch family, in turn, is closely associated with the development of cancer stem cells [21] and plays an important role in a variety of cancers such as liver [22], breast [23], and thyroid [24] cancers as well as colorectal cancer [25]. In colorectal cancer, JAG1 regulates the development of the cancers by binding to Notch. Chen et al. showed that the JAG1/Notch2 pathway can activate the EMT process and regulate the invasive metastatic ability of colorectal cancer [26]. Pelullo et al. showed that JAG1 plays an important role in regulating the development and drug resistance of colorectal cancer cells [27]. In this study, Co-IP experiments conducted in HCT8 and HCT116 cell lines have confirmed the interaction between JAG1 and NOTCH1 (Fig. S2G), suggesting that JAG1 might regulate the radiosensitivity of CRC by modulating cellular stemness. External research supports this by demonstrating that Sec62 significantly influences CRC stemness, notably through enhancing β-catenin signaling via its BCBL motif, and acts as a crucial β-catenin activator in CRC, irrespective of APC mutation status or the presence of Wnt signaling [28]. The importance of β-catenin signaling and stemness in cancer progression and treatment resistance further underscores the potential role of JAG1 within this regulatory network. Although the direct involvement of JAG1 in modulating CRC radiosensitivity has not been established in other studies, our experiments show that knocking down JAG1 expression in cancer cells, followed by irradiation, significantly augmented their radiation resistance. However, the exact mechanism by which JAG1 regulates CRC radiosensitivity through stemness requires further experimental validation.

In addressing a critical clinical challenge, this study sheds light on the modulation of radiosensitivity in CRC. It was found that radiation exposure significantly upregulates miR-199b-5p in exosomes secreted by cancer-associated adipose tissue, a key factor in this process. These miR-199b-5p-rich exosomes contribute to reduced intracellular JAG1 expression, thereby enhancing radioresistance in CRC cells (Fig. 5). The study proposes a novel axis, with adipocyte-derived exosomes secreting miR-199b-5p targeting JAG1, elucidating the mechanism governing radiosensitivity modulation. Notably, the research confirms the significant upregulation of miR-199b-5p in exosomes following radiation, emphasizing the sophisticated nature of cell-to-cell communication via exosome secretion in the tumor microenvironment. However, limitations are evident, primarily in the need for further exploration of the detailed mechanisms. Critical areas for future research include understanding how miR-199b-5p, upregulated by irradiation from diverse sources, competes and interacts within cancer cells. Furthermore, while the focus was on the miR-199b-5p/JAG1 axis in CRC radiosensitivity, the potential for other regulatory pathways and target genes of miR-199b-5p warrants investigation. These findings underscore the importance of comprehensive experiments to unravel the complex molecular interplay in CRC radiosensitivity.

In conclusion, our study elucidates the regulatory role of adipocyte-derived exosomes in the radiosensitivity of colorectal cancer. miR-199b-5p induces radioresistance of colorectal cancer by targeting JAG1. These results provide new insights into the mechanisms by which adipocytes regulate the radiosensitivity of colorectal cancer and offer potential avenues for radiotherapy intervention in colorectal cancer.

Ethics statement

The present study was approved by Ethics Committee of Soochow University (approval no. SUDA20221024A02), and was performed according to the guidelines of the Committee on Animal Research and Ethics.

Funding

This study was supported by the National Natural Science Foundation of China (No. 82003219, 82073476, and 81773226), the

National key R&D Program of China (2022YFC2503700, 2022YFC2503703), the Suzhou Science and Technology Development Project (SYS2019059), the Key scientific research projects of Jiangsu Provincial Health Commission (ZD2021053), the Wuxi double hundred young and middle-aged medical and health top-notch talent project (No. 202014), the Project of State Key Laboratory of Radiation Medicine and Protection (czc00402, CZN1202101), the Project of Scientific and Technological Innovation of Nuclear Medicine (ZHYLYB2021012, ZHYLZD2021004), the Research project of China Baoyuan Investment Co., Ltd., and the Scientific Research Program for Young Talents of China National Nuclear Corporation.

Data availability statement

The data that support the findings of this study are available from the corresponding author upon reasonable request.

CRediT authorship contribution statement

Xiaoli Lv: Writing – original draft, Formal analysis, Data curation, Conceptualization. **Zhenyan Li:** Formal analysis, Data curation. **Yunpeng Dai:** Formal analysis, Data curation. **Yuji Xiao:** Methodology. **Fangrong Shen:** Methodology. **Jian Wang:** Methodology. **Jianping Cao:** Supervision, Resources. **Lili Wang:** Writing – review & editing, Conceptualization. **Qiliang Peng:** Writing – review & editing, Data curation. **Yang Jiao:** Writing – review & editing, Project administration, Conceptualization.

Declaration of competing interest

The authors declare that they have no known competing financial interests or personal relationships that could have appeared to influence the work reported in this paper.

Appendix A. Supplementary data

Supplementary data to this article can be found online at https://doi.org/10.1016/j.heliyon.2024.e24412.

References

[1] International Agency for Research on Cancer [cited 2022 March 4]; Colorectum cancer]. Available from: https://gco.iarc.fr/today/online-analysis-pie-colorectum, 2022.
[2] L.H. Biller, D. Schrag, Diagnosis and treatment of metastatic colorectal cancer: a review, JAMA 325 (7) (2021) 669–685.
[3] G. Tan, et al., Radiosensitivity of colorectal cancer and radiation-induced gut damages are regulated by gasdermin, E. Cancer Lett 529 (2022) 1–10.
[4] S.S. Vispute, et al., The effect of abdominal exercise on abdominal fat, J Strength Cond Res 25 (9) (2011) 2559–2564.
[5] K.M. Nieman, et al., Adipocytes promote ovarian cancer metastasis and provide energy for rapid tumor growth, Nat Med 17 (11) (2011) 1498–1503.
[6] B. Dirat, et al., Cancer-associated adipocytes exhibit an activated phenotype and contribute to breast cancer invasion, Cancer Res. 71 (7) (2011) 2455–2465.
[7] S. Wang, et al., Exosomes released by hepatocarcinoma cells endow adipocytes with tumor-promoting properties, J. Hematol. Oncol. 11 (1) (2018) 82.
[8] J. Nie, et al., Adipocytes promote cholangiocarcinoma metastasis through fatty acid binding protein 4, J. Exp. Clin. Cancer Res. 36 (1) (2017) 183.
[9] D.M. Pegtel, S.J. Gould, Exosomes, Annu. Rev. Biochem. 88 (2019) 487–514.
[10] L. Zhang, D. Yu, Exosomes in cancer development, metastasis, and immunity, Biochim. Biophys. Acta Rev. Canc 1871 (2) (2019) 455–468.
[11] S. Zhao, et al., Tumor-derived exosomal miR-934 induces macrophage M2 polarization to promote liver metastasis of colorectal cancer, J. Hematol. Oncol. 13 (1) (2020) 156.
[12] Z. Sun, et al., Effect of exosomal miRNA on cancer biology and clinical applications, Mol. Cancer 17 (1) (2018) 147.
[13] Y. Zhou, et al., Luminescent ruthenium(II) polypyridyl complexes acted as radiosensitizer for pancreatic cancer by enhancing radiation-induced DNA damage, Theranostics 9 (22) (2019) 6665–6675.
[14] Y. Xu, et al., Disulfiram alone functions as a radiosensitizer for pancreatic cancer both in vitro and in vivo, Front. Oncol. 11 (2021) 683695.
[15] Y. Feng, et al., METTL3 Mediates epithelial-mesenchymal transition by modulating FOXO1 mRNA N(6) -Methyladenosine-Dependent YTHDF2 binding: a novel mechanism of radiation-induced lung injury, Adv. Sci. 10 (17) (2023) e2204784.
[16] A.J. Hoy, S. Balaban, D.N. Saunders, Adipocyte-tumor cell metabolic crosstalk in breast cancer, Trends Mol. Med. 23 (5) (2017) 381–392.
[17] Q. Wu, et al., Cancer-associated adipocytes: key players in breast cancer progression, J. Hematol. Oncol. 12 (1) (2019) 95.
[18] Z. Zhao, et al., miR-199b-5p-DDR1-ERK signalling axis suppresses prostate cancer metastasis via inhibiting epithelial-mesenchymal transition, Br. J. Cancer 124 (5) (2021) 982–994.
[19] S. Chen, et al., MiR-199b-5p promotes gastric cancer progression by regulating HHIP expression, Front. Oncol. 11 (2021) 728393.
[20] Z. Liu, et al., miR-6716-5p promotes metastasis of colorectal cancer through downregulating NAT10 expression, Cancer Manag. Res. 11 (2019) 5317–5332.
[21] S.A. Ibrahim, et al., Syndecan-1 is a novel molecular marker for triple negative inflammatory breast cancer and modulates the cancer stem cell phenotype via the IL-6/STAT3, Notch and EGFR signaling pathways, Mol. Cancer 16 (1) (2017) 57.
[22] Y.C. Ye, et al., NOTCH signaling via WNT regulates the proliferation of alternative, CCR2-independent tumor-associated macrophages in hepatocellular carcinoma, Cancer Res. 79 (16) (2019) 4160–4172.
[23] A. Nandi, R. Chakrabarti, The many facets of Notch signaling in breast cancer: toward overcoming therapeutic resistance, Genes Dev. 34 (21–22) (2020) 1422–1438.
[24] R. Guenter, Z. Patel, H. Chen, Notch signaling in thyroid cancer, Adv. Exp. Med. Biol. 1287 (2021) 155–168.
[25] R. Jackstadt, et al., Epithelial NOTCH signaling rewires the tumor microenvironment of colorectal cancer to drive poor-prognosis subtypes and metastasis, Cancer Cell 36 (3) (2019) 319–336 e7.
[26] J. Chen, et al., miR-598 inhibits metastasis in colorectal cancer by suppressing JAG1/Notch2 pathway stimulating EMT, Exp. Cell Res. 352 (1) (2017) 104–112.
[27] M. Pelullo, et al., Kras/ADAM17-Dependent jag1-ICD reverse signaling sustains colorectal cancer progression and chemoresistance, Cancer Res. 79 (21) (2019) 5575–5586.
[28] X. Liu, et al., Sec62 promotes stemness and chemoresistance of human colorectal cancer through activating Wnt/beta-catenin pathway, J. Exp. Clin. Cancer Res. 40 (1) (2021) 132.